


Cite this: *RSC Adv.*, 2021, 11, 24183

# Nylon membranes modified by gold nanoparticles as surface-enhanced Raman spectroscopy substrates for several pesticides detection†

Haitao Yu,<sup>a</sup> Qian Lyu,<sup>a</sup> Xueli Chen,<sup>ab</sup> Dongyi Guo,<sup>a</sup> Dingping He,<sup>a</sup> Xiwen Jia,<sup>a</sup> Lujia Han<sup>a</sup> and Weihua Xiao<sup>\*a</sup>

Surface enhanced Raman spectroscopy (SERS) is an attractive means for trace compound detection because of its high sensitivity, however, the poor reproducibility is a major challenge. Herein, we propose a facile SERS strategy employing the several developed test processes to improve the repeatability of the SERS analysis based on regular nylon membranes as substrates to detect trace compounds. Various methods, including *in situ* reduction, immersion adsorption, and filtration, were first compared to prepare composite substrates using nylon membranes and gold nanoparticles. The substrates prepared by filtration showed the best test parallelism (RSD = 7.85%). Its limit of detection (LOD) could reach  $10^{-8}$  g mL<sup>-1</sup> with a good linear relationship in the range  $10^{-8}$  to  $10^{-7}$  g mL<sup>-1</sup>. Finally, three pesticide solutions were tested to verify the substrate applicability. A superior LOD of  $10^{-8}$  g mL<sup>-1</sup> was observed for thiram, whereas the LODs of both phorate and benthocarb could reach  $10^{-6}$  g mL<sup>-1</sup>. Overall, modifying nylon membrane substrates with gold nanoparticles improves the repeatability and economic viability of SERS and favors its wider commercial application for detecting trace compounds.

Received 5th May 2021  
Accepted 23rd June 2021

DOI: 10.1039/d1ra03490a

rsc.li/rsc-advances

## Introduction

Surface enhanced Raman scattering, the increased Raman scattering signal caused by the adsorption of molecules on rough plasmonic metal nanoparticles,<sup>1</sup> has been well developed in recent years. Gold and silver nanoparticles have good localized surface plasmon resonance (LSPR)<sup>2,3</sup> and are the most commonly used materials.<sup>4,5</sup> Compared with traditional analysis methods, SERS has the advantages of being nondestructive and allowing for fast detection for trace compounds.<sup>6</sup> The SERS enhancement factor can reach  $10^5$  to  $10^6$  and this can be attributed to the chemical and electromagnetic enhancement afforded by the metal nanoparticles.<sup>7</sup>

With growing environmental concerns, the fast detection of trace pollutants such as pesticides, dyes, and antibiotics using SERS has attracted growing attention.<sup>8,9</sup> Although nanoparticles in colloidal solution can be easily obtained for SERS analysis,<sup>10</sup> the distribution of “hot spots” is not controllable and uniform, which affects the reproducibility in practical application. Various types of

SERS substrates have been designed to improve uniformity, stability, and sensitivity *via* immobilization of gold or silver nanoparticles on rigid or flexible substrates.<sup>11</sup> For this, electron beam etching,<sup>12</sup> electron beam evaporation,<sup>13</sup> or interface deposition methods<sup>14</sup> have been employed for SERS substrate fabrication. However, most of these methods are complicated and the substrates are costly. Compared with the rigid substrate, paper-based or membrane-based substrates have the superiorities of portability, low cost, and simple operation, possessing the potential for practical SERS applications.<sup>15,16</sup>

Standardization of testing methods is necessary to reliably bring the technology to market.<sup>17,18</sup> However, most reports on flexible substrates provide LODs (limits of detection) of the extract analyte using unique test methods, and it is rare to see comparative studies of the different test methods. Fateixa and co-workers developed a SERS active substrate (Ag/LCP) based on liquid-crystal polymer (LCP) textile fibers decorated with Ag NPs, which has satisfactory LODs for thiram (0.024 ppm).<sup>19</sup> It still needs two steps to prepare the substrates and enrich the analyte for detection. To obtain a fast and reliable SERS test method, we compared a colloidal test solution and several nylon membrane substrates immobilized with Au NPs. The sample loading method, which included the immersion and drop tests, was also investigated. The stability, repeatability, and LODs of the test were determined, and the enhancement mechanisms are explained *via* appropriate characterization methods.

<sup>a</sup>College of Engineering, China Agricultural University (East Campus), Box 191, Beijing 100083, China. E-mail: xwhddd@163.com; Fax: +86 10 62736778; Tel: +86 10 62736778

<sup>b</sup>Laboratory of Renewable Resources Engineering, Department of Agricultural and Biological Engineering, Purdue University, West Lafayette, Indiana 47907, USA

† Electronic supplementary information (ESI) available. See DOI: 10.1039/d1ra03490a



## Materials and methods

### Materials

The following materials were used as purchased: nylon membrane (0.1 mm pore diameter, Shanghai Xingya purification material factory); glass dish (10 mm diameter, Shanghai JingAn Biological Science and Technology Ltd.); chloroauric acid ( $\text{HAuCl}_4$ , Macklin) sodium citrate tribasic dihydrate ( $\text{Na}_3\text{C}_6\text{H}_5\text{O}_7 \cdot 2\text{H}_2\text{O}$ , 99%, Macklin); *p*-aminophenol (4-ATP, 97%, Macklin); thiram (99.2%, Beijing Zhongjian Navigation Mark Metering Technology Co. Ltd); phorate (100  $\mu\text{g mL}^{-1}$ , 95.9%, Beijing Zhongjian Navigation Mark Metering Technology Co. Ltd); benthocarb (98.1%, Dr Ehrenstorfer GmbH). The water was obtained from a Milli-Q system. Au NPs were synthesized *via* the sodium citrate reduction method, which was modified by Frens *et al.*<sup>20</sup> (details in the ESI†).

### Nylon membrane composite substrates

*In situ* reduction substrates (NL-R group): the nylon membrane was cut into small pieces and soaked in a chloroauric acid solution and then boiled. After adding  $\text{Na}_3\text{Cit} \cdot 2\text{H}_2\text{O}$  for a period of time, the reduction reaction was terminated. Finally, the nylon membrane was taken out and air-dried.

Immersion adsorption-substrates (NL-A group): the nylon membrane was completely immersed in the prepared Au NPs solution for 24 h for sufficient adsorption. Then, they were air-dried for testing.

Filtration-substrates (NL-F group): for filtration using a purchased nylon membrane, the red color of the Au NPs disappeared. Filtration was stopped when the color reappeared in the filtrate, which indicated that the largest amount of Au NPs was trapped in the nylon membrane. Then, the filtered membrane was air dried for testing.

### Characterization methods

The morphology of the Au NPs filtration substrates were characterized by the field emission scanning electron microscopy (SEM) (Hitachi, SU8020) and the atomic force microscopy (AFM) (Bruker, Multimode 8). The charged property of the surface of the gold nanoparticles ( $\text{pH} = 4.16 \pm 0.02$ ) was determined using

a Zeta potentiometer (Malvern, Zetasizer Nano). Ultraviolet-visible light spectroscopy (UV-Vis) was used to characterize the Au NP surface plasmon resonance (SPR) information. The FDTD solutions software was used as the simulation software to investigate the enhancement effect with the Au NPs.

### Acquisition and pre-processing of the SERS

The SERS were acquired using a confocal Raman spectral system (Bruker, SENTERRA II). Before analysis, methanol solutions of 4-ATP with concentrations between  $10^{-4}$  g  $\text{mL}^{-1}$  and  $10^{-8}$  g  $\text{mL}^{-1}$  were prepared. The Au NPs were mixed with the sample at a volume ratio of 1 : 1 and 100  $\mu\text{L}$  of the mixed liquid was added to a clean glass dish ( $\Phi = 10$  mm) for testing; this sample is referred to as the L group. The air-dried filtration-substrates were fixed on the glass slide. Then, the sample (100  $\mu\text{L}$ ) was dropped on the substrates and air-dried for testing (referred to as the drop-test sample). The air-dried filtration-substrates were immersed in the sample (1.5 mL) for 480 min for full adsorption. The substrates were then removed and air dried (referred to as the immersion-test samples). The air-dried filtration-substrates were cut into  $\Phi 13$  and were put in the corresponding removable filter. Then the sample (5 mL) was filtered through the substrates and air-dried for testing (referred to as the filter-test sample). The laser power was 100 mW for the L group and 10 mW for the drop-test, the immersion-test and the filter-test sample. Specific test conditions were showed in the ESI.†

### Detection of the pesticides

Before analysis, methanol solutions of thiram with concentrations between  $10^{-7}$  g  $\text{mL}^{-1}$  and  $10^{-8}$  g  $\text{mL}^{-1}$  were prepared. The methanol solutions of phorate and benthocarb with concentrations between  $10^{-5}$  g  $\text{mL}^{-1}$  and  $10^{-6}$  g  $\text{mL}^{-1}$  were prepared as well. The acquisition of SERS spectrum was consistent with the filter-test sample as mentioned above.

### Data analysis

After baseline correction and smoothing of spectral data by system software (Bruker, SENTERRA II), the calibration curves were generated by monitoring the intensity of the band at

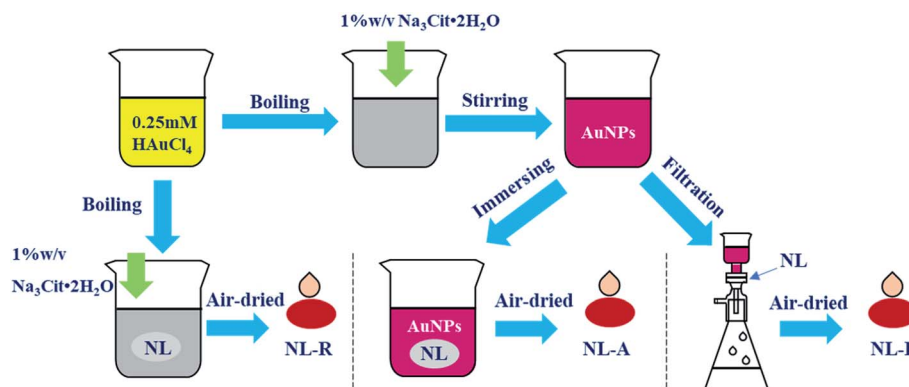


Fig. 1 Preparation of several SERS substrates.



1080  $\text{cm}^{-1}$  (C–S bond) and 1588  $\text{cm}^{-1}$  (C–C bond) as a function of analyte concentration. Each point on the calibration curve represents the average value of Raman measurements with error bars representing the standard deviation. The coefficient of determination ( $R^2$ ) for each calibration curve was calculated using the Excel. The figures were described by Origin 8.

## Results and discussion

### Characterization of the filtration-substrates and the Au NPs

The surface plasmon resonance peak of the Au NPs in the UV-Vis spectrum was at 535.3 nm (Fig. S1†). Considering the study of Haiss *et al.*,<sup>21</sup> it could be calculated that the concentration was  $\sim 0.0593$  nM. The  $\zeta$ -potential values for the Au NPs was affected by the added citrate and determined to be  $-23.4 \pm 4.4$  mV, and the surface was negatively charged. This electrostatic phenomenon results in mutual repulsion of the Au NPs in the colloid and enables a stabilized suspension, which extends their preservation time.<sup>22</sup> When the analyte was mixed with the Au NPs for testing, the introduction of the analyte would destroy the electrical equilibrium in the solution to a certain extent.<sup>23,24</sup> The color of the solution then changed from red to gray as the Au NPs aggregated, resulting in the formation of “hot spots”.<sup>25</sup> FDTD simulations can theoretically explain the enhancement of the electric field around the Au NPs.<sup>26,27</sup> From the simulation results (Fig. S2 and S3†), it can be seen that a smaller distance between the particles results in a larger electric field enhancement. The Raman scattering signal was positively correlated with the electric field enhancement. Therefore, increased aggregation is conducive to signal enhancement. It is difficult to control the aggregation process of Au NPs. The aggregates undergo Brownian motion<sup>28</sup> and are randomly distributed in the mixed solution, which decreases the reproducibility of the test. Finally, this leads to the high RSD value and poor reproducibility, which means that it cannot be used as a reliable quantitative detection method. If measurements are carried out after the mixture is air-dried in the cell culture dish, the “coffee ring” phenomenon occurs,<sup>29</sup> which is conducive to reducing the

LODs. However, there remains the issue of poor reproducibility and a time-consuming experimental procedure for quantitative analysis (Fig. 1).

The distribution of the Au NPs on the nylon membrane after filtering and air-drying is shown in Fig. 2. The Au NPs are uniformly attached to the surface of the nylon fiber, and there is a certain interval between the particles and the formation of a considerable number of “hot spots”. The main component of nylon membrane is polyamide, which contains carbon chains of different lengths and aromatic rings, and the main functional groups are  $-(\text{CH}_2)_n-$  and  $-\text{NH}-\text{CO}-$ . Hydrogen bonds, which are both hydrophilic and hydrophobic, can be easily formed. Because the surface of nylon fiber is positively charged, it can trap the Au NPs *via* electrostatic adsorption. Compared with the liquid test (L group), the filtration substrates trap the increased “hot spots” on the nylon fiber, reducing randomness in the measurement caused by motion of the “hot spots”. This can decrease the RSD value and enable quantitative analysis.

### SERS measurement of several nylon membrane composite substrates and Au NPs

The standard spectra of 4-ATP were investigated using the pressed disc method, and the results are shown in Fig. 3. Characteristic peaks can be observed at 1080  $\text{cm}^{-1}$  (C–S bond) and 1588  $\text{cm}^{-1}$  (C–C bond), which could be observed in the SERS measurements as well. The SERS sensitivity of the Au NPs for detection of 4-ATP can be seen in Fig. S4.† In this experiment, 4-ATP was loaded in the mixture and then analyzed *via* SERS (785 nm laser). Methanol was used instead of water because 4-ATP is more soluble in methanol.<sup>19</sup> Although the methanol has very defined Raman bands (1020  $\text{cm}^{-1}$ ), the SERS substrates were air dried after being in contact with the 4-ATP methanol solution and no Raman bands could be observed for methanol. Additionally, the Raman signals at the different wavenumbers did not affect each other. The relative standard deviation (RSD) of the characteristic peak was calculated to determine the reproducibility of the method. The RSD values

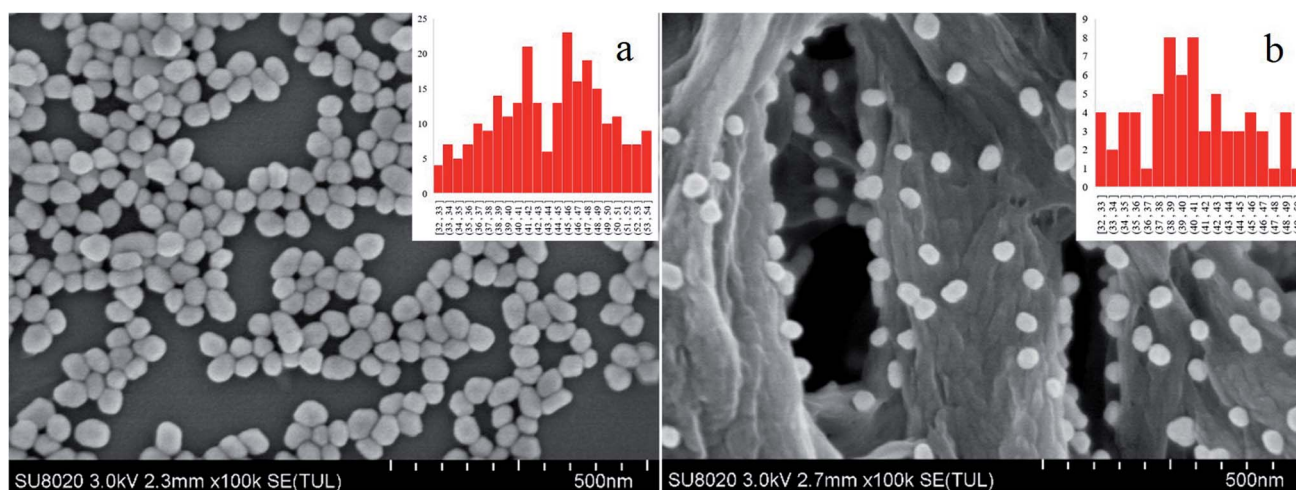


Fig. 2 SEM characterization of gold nanoparticles (a) and the filtration substrates (b).

were high for the signals at both 1080 and 1588  $\text{cm}^{-1}$ , demonstrating poor reproducibility. Table 1 shows the RSD values of several nylon membrane composite substrates. The filtration-substrates (NL-F group) had the smallest RSD value in the groups (Fig. 4) at 7.85%, and the error between the groups was 1.77%, indicating that the preparation method for this substrate was relatively stable. Therefore, the filtration-substrates have better reproducibility and are more suitable for quantitative analysis than the adsorption substrates (NL-A group) and the *in situ* reduction substrates (NL-R group). The analytical results in Fig. 5a show that the spectral intensity at both characteristic peaks had a good linear correlation with the solution concentration in the range  $10^{-5}$  to  $5 \times 10^{-4}$   $\text{g mL}^{-1}$ , suggesting that the established filtration-substrates can be applied for quantitative trace detection of 4-ATP.

### Comparison among three test methods

After the preparation and selection of the substrates, the different test methods were investigated. Compared with the drop test, the immersion test had a larger enhancement of the Raman intensity for the same 4-ATP concentration. The drop-test method has a characteristic peak signal at a concentration of  $10^{-6}$   $\text{g mL}^{-1}$ , while the immersion test had a signal at a concentration of  $10^{-7}$   $\text{g mL}^{-1}$ , which is almost an order of magnitude lower than the drop test. The analytical results of the immersion tests in Fig. 5b show that the spectral intensity at both characteristic peaks had a good linear correlation with the solution concentration in the range of  $10^{-7}$  to  $10^{-6}$   $\text{g mL}^{-1}$ . The mercapto group of 4-ATP has specific adsorption to the Au NPs.<sup>30</sup> In the drop test, the drop volume of the analyte was only 100  $\mu\text{L}$ , and the number of molecules to be measured per unit area was much less than that for the immersion test. Therefore, the immersion-test has a lower LOD.

To reduce the test time, we investigated the influence of the immersion time on the SERS intensity of 4-ATP. Fig. S7† shows

Table 1 RSD value of several different substrates

Characteristic peak ( $\text{cm}^{-1}$ )	L (%)	NL-R (%)	NL-A (%)	NL-F (%)	NL-F (between group) (%)
1080	19.66	33.35	10.49	8.03	4.46
1588	25.34	33.66	10.36	7.85	1.77

the intensity of the characteristic peak at different concentrations and for different immersion times. It can be seen that with increasing time, the measured SERS intensity increased and then tended to stabilize. During the immersion process, the 4-ATP molecule adsorbed on the Au NPs trapped on the nylon membrane, and the characteristic peak intensity can represent the number of adsorbed molecules. For adsorption durations >480 min, the SERS intensity remained basically stable and did not increase, which indicated adsorption saturation. The signal was not observable until 30 min after adsorption with  $10^{-7}$   $\text{g mL}^{-1}$  4-ATP. Therefore, for quantitative analysis, immersion for a sufficient period of time is necessary. The consumption of time makes this test method not fast enough to show the advantage in detection.

The filter tests can reduce the test time through filtration operations, while reducing the detection limit due to forced enrichment. The analytical results of the filter tests in Fig. 5c show that the spectral intensity at both characteristic peaks had a good linear correlation with the solution concentration in the range of  $10^{-8}$  to  $10^{-7}$   $\text{g mL}^{-1}$ . The LOD was  $10^{-8}$   $\text{g mL}^{-1}$  ( $S/N > 3$ ).

### Filter tests for different pesticides detection

As a newly developed test method, SERS has been applied in many fields, especially for medical monitoring and environmental pollutant detection. Thiram, phorate and benthocarb are often used in the cultivation of rice, vegetables and fruits. The residues of these pesticides threaten food safety and cause environmental pollution.<sup>31,32</sup> Compared with traditional detection methods such as liquid mass spectrometry (LC-MS) and gas mass spectrometry (GC-MS), the method proposed in this study has advantages of fast, efficient and low cost. Therefore, the detection of the pesticides was evaluated. As shown in Fig. 6a, thiram has a characteristic peak at 1380  $\text{cm}^{-1}$ ; phorate has a characteristic peak at 630  $\text{cm}^{-1}$  and benthocarb has a characteristic peak at 1264  $\text{cm}^{-1}$ . The intensity of the SERS all had a good linear correlation with the solution concentration which was shown in Fig. 6b–d. According to the criterion of the LOD, the signal can still be detected at the concentration of  $10^{-8}$   $\text{g mL}^{-1}$  for thiram, while  $10^{-6}$   $\text{g mL}^{-1}$  for both phorate and benthocarb ( $S/N > 3$ ). In the future, expansion of the analyte range and test conditions will need to be supplemented by further research.

### Comparison of various test substrates based on SERS

With the continued development of the SERS technique, a variety of advanced substrate materials have been reported in laboratory research. Commonly used AuNPs<sup>33</sup> and AgNPs<sup>34</sup> are

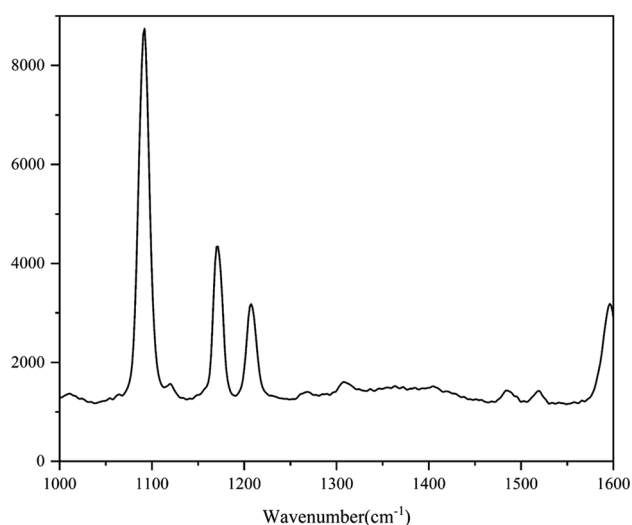


Fig. 3 Raman spectra of 4-ATP (excitation wavelength: 785 nm; laser power: 100 mW).





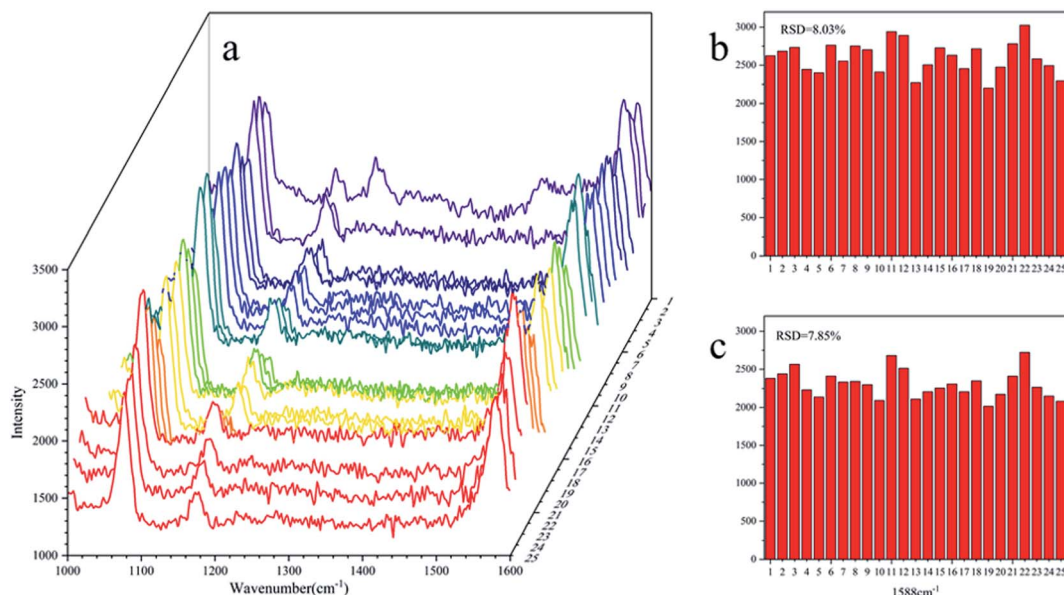


Fig. 4 RSD value of the NL-F group with the drop test ((a): SERS spectra of 25 tests; (b): RSD value at  $1080\text{ cm}^{-1}$ ; (c): RSD value at  $1588\text{ cm}^{-1}$ ).

suitable for qualitative analysis, and the heterogeneity of “hot spots” in the solution results in high RSD values. To ensure uniformity of the tests, commercial substrates are prepared *via* photolithography<sup>35</sup> or interfacial deposition.<sup>36</sup> The controllability of the metal organic framework<sup>37</sup> greatly improves the uniformity of the measurements. The addition of molecularly

imprinted polymers<sup>38</sup> also allows for specific detection and reduces the LOD. However, the preparation of these substrates is a very complex and expensive process. Applications in biological or screening tests (such as cancer cells or COVID-19) could justify the cost of these substrates, but the cost for applications such as water pollution testing would be

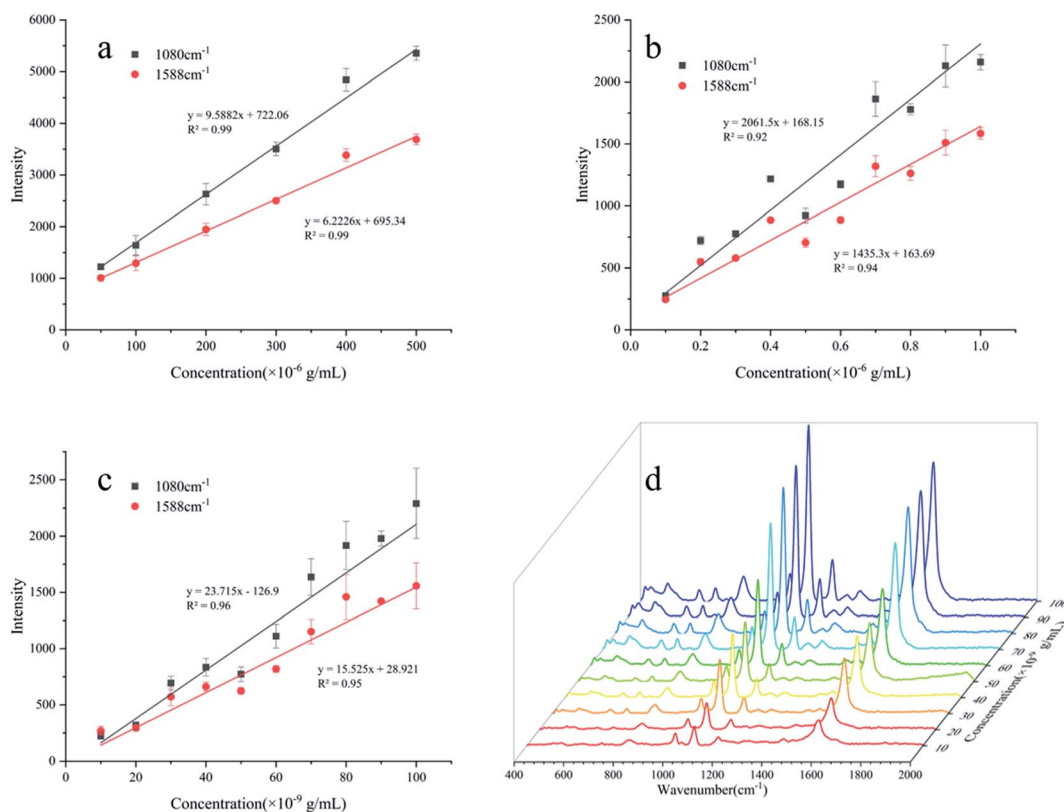


Fig. 5 Quantitative analysis of the NL-F group by three different test methods ((a): the drop-test; (b): the immersion-test; (c): the filter-test; (d): SERS of the filter-test between  $10^{-8}$  to  $10^{-7}\text{ g mL}^{-1}$  4-ATP).

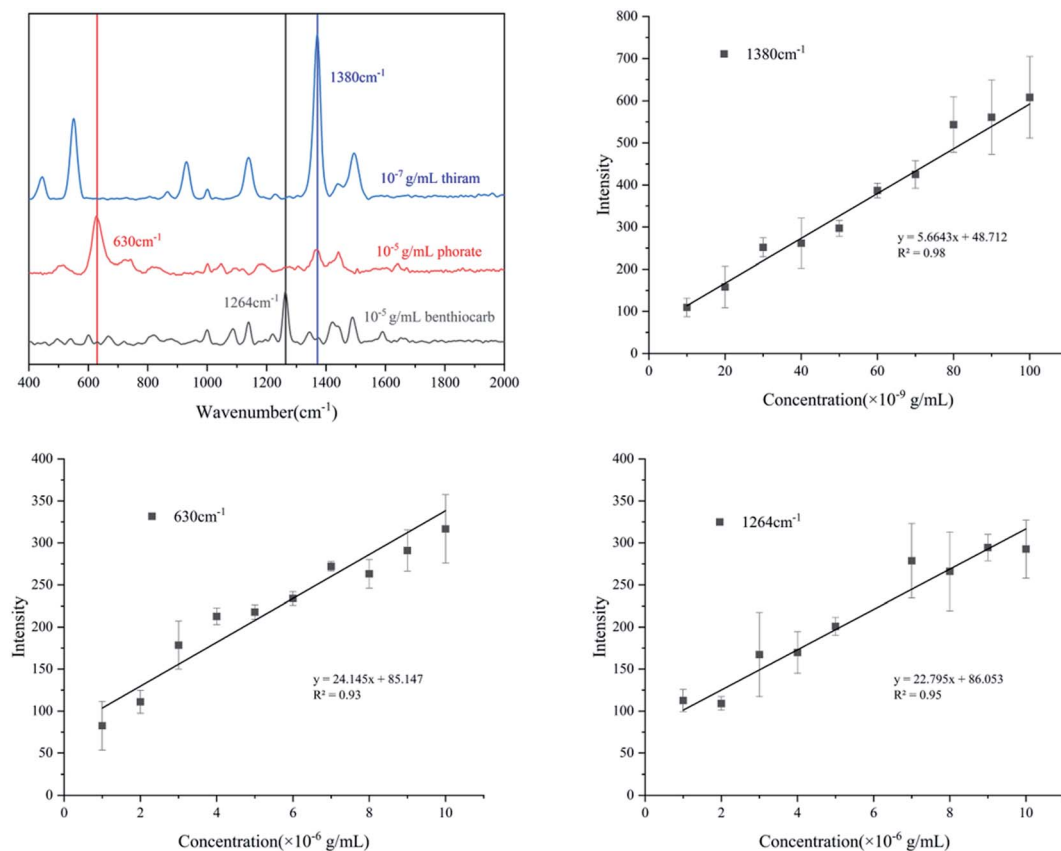


Fig. 6 Quantitative analysis of three different pesticides ((a): characteristic peak selection; (b): thiram; (c): phorate; (d): benthocarb).

Table 2 Comparison of various test substrates based on SERS

Pesticides	Substrates	LODs (g mL <sup>-1</sup> )	Range of linearity (g mL <sup>-1</sup> )	Reference
Thiram	AuNR@Ag substrate	$2.41 \times 10^{-8}$	—	Pastorello, <i>et al.</i> , 2020 (ref. 39)
Thiram	PMMA/AgNP/graphene substrate	$2.41 \times 10^{-7}$	—	Sun, <i>et al.</i> , 2017 (ref. 40)
Phorate	Ag dendrites/aptamer substrate	$1.04 \times 10^{-8}$	0 to $9.89 \times 10^{-4}$	Pang, <i>et al.</i> , 2014 (ref. 41)
Chlorpyrifos	AgNPs	$3.51 \times 10^{-10}$	$3.51 \times 10^{-4}$ to $3.51 \times 10^{-10}$	Ma, <i>et al.</i> , 2020 (ref. 34)
R6G	AuNP substrate with hydrogen peroxide treatment	$2.21 \times 10^{-9}$	—	Gorbachevskii, <i>et al.</i> , 2018 (ref. 42)
Various opiates median	AuNP substrate	$5 \times 10^{-11}$	—	Ding, <i>et al.</i> , 2020 (ref. 37)
Imidacloprid	Paper + 3D silver dendrites + MIP	$2.81 \times 10^{-11}$	$2 \times 10^{-10}$ to $8 \times 10^{-7}$	Zhao, <i>et al.</i> , 2020 (ref. 38)
Thiram	Nylon membrane modified by gold nanoparticles	$10^{-8}$	$10^{-7}$ to $10^{-8}$	This work
Phorate		$10^{-6}$	$10^{-5}$ to $10^{-6}$	
Benthocarb		$10^{-6}$	$10^{-5}$ to $10^{-6}$	

unfeasible. Because of the complexity of the variables, most of the methods cannot be used in unstable environments outside the laboratory. This makes it difficult to translate these research methods into practical applications as well.

Therefore, low-cost paper-based or membrane-based substrates are one of the avenues for such tests.<sup>21,22</sup> In this study, the filtration-substrates were used for SERS measurements. A deviation in the characteristic peak intensity was observed between test batches. The substrates had almost similar LODs as the commercial substrates. The issue with test uniformity was addressed using a very low-cost commercial

nylon membrane combined with a simple filtration method, however, this process sacrificed the “hot spots”. This loss was compensated for by using the filter test. The suitable test uniformity and LODs reflect the advantages of the filtration substrates (Table 2).

## Conclusion

To find a low-cost and reliable SERS testing strategy for qualitative and quantitative analysis of trace compounds, we used a nylon membrane to trap Au NPs *via* filtration. The



reproducibility was considered for several nylon membrane composite substrates. The results showed that the filtration substrates had a lower RSD value, which indicated viability for quantitative analysis. Further investigation showed that the filter test had a better LOD ( $10^{-8}$  g mL $^{-1}$ ) and a good linear correlation within the range of  $10^{-7}$  to  $10^{-8}$  g mL $^{-1}$  for 4-ATP. Three pesticides were investigated to explore the applications. The LOD of thiram was  $10^{-8}$  g mL $^{-1}$ , while both phorate and benthocarb could reach  $10^{-6}$  g mL $^{-1}$ . This study demonstrated a facile SERS testing process for trace compounds with good stability and repeatability. In the future, further studies are needed to expand detection to a variety of compounds.

## Conflicts of interest

There are no conflicts to declare.

## Acknowledgements

This work was supported by the National Key R&D Program of China (No. 2016YFE0112800) and the Innovation Team Project of the Education Ministry (No. IRT\_17R105).

## References

- 1 B. Sharma, R. R. Frontiera, A. I. Henry, E. Ringe and R. P. Van Duyne, *Mater. Today*, 2012, **15**, 16–25.
- 2 N. G. Bastus, J. Comenge and V. Puentes, *Langmuir*, 2011, **27**, 11098–11105.
- 3 A. Gole and C. J. Murphy, *Chem. Mater.*, 2004, **16**, 3633–3640.
- 4 X. Chen, M. Lin, L. Sun, T. Xu, K. Lai, M. Huang and H. Lin, *Food Chem.*, 2019, **293**, 271–277.
- 5 H. Zhao, D. Huang and S. Zhu, *Sensors*, 2019, **19**, 5354.
- 6 W. E. Smith, *Chem. Soc. Rev.*, 2008, **37**, 955–964.
- 7 P. A. Mosier-Boss, *Nanomaterials*, 2017, **7**, 142.
- 8 A. Marques, B. Veigas, A. Araújo, B. Pagará, P. V. Baptista, H. Águas, R. Martins and E. Fortunato, *Sci. Rep.*, 2019, **9**, 17922.
- 9 F. Fu, B. Yang, X. Hu, H. Tang, Y. Zhang, X. Xu, Y. Zhang, S. S. B. Touhid, X. Liu, Y. Zhu, J. Zhou and J. Yao, *Chem. Eng. J.*, 2020, **392**, 123693.
- 10 T. Yaseen, D. W. Sun, H. Pu and T. T. Pan, *Food Anal. Methods*, 2018, **11**, 2518–2527.
- 11 L. B. Zhong, Q. Liu, P. Wu, Q. F. Niu, H. Zhang and Y. M. Zheng, *Environ. Sci. Technol.*, 2018, **52**, 5812–5820.
- 12 N. A. A. Hatab, J. M. Oran and M. J. Sepaniak, *ACS Nano*, 2008, **2**, 377–385.
- 13 J. L. Abell, J. D. Driskell, R. A. Dluhy, R. A. Tripp and Y.-P. Zhao, *Biosens. Bioelectron.*, 2009, **24**, 3663–3670.
- 14 H. Duan, D. Wang, D. G. Kurth and H. Mohwald, *Angew. Chem., Int. Ed.*, 2004, **43**, 5639–5642.
- 15 K. Oh, M. Lee, S. G. Lee, D. H. Jung and H. L. Lee, *Cellulose*, 2018, **25**, 3339–3350.
- 16 W. Wu, L. Liu, Z. Dai, J. Liu, S. Yang, L. Zhou, X. Xiao, C. Jiang and V. A. L. Roy, *Sci. Rep.*, 2015, **5**, 10208.
- 17 S. Pang, T. Yang and L. He, *TrAC, Trends Anal. Chem.*, 2016, **85**, 73–82.
- 18 A. Jaworska, S. Fornasaro, V. Sergo and A. Bonifacio, *Biosensors*, 2016, 647.
- 19 S. Fateixa, M. Raposo, H. I. S. Nogueira and T. Trindade, *Talanta*, 2018, **182**, 558–566.
- 20 G. Frens, *Nat. Phys. Sci.*, 1973, **241**, 20–22.
- 21 W. Haiss, N. T. K. Thanh, J. Aveyard and D. G. Fernig, *Anal. Chem.*, 2007, **79**, 4215–4221.
- 22 N. G. Bastus, J. Comenge and V. Puentes, *Langmuir*, 2011, **27**, 11098–11105.
- 23 L. Xie, J. Lu, T. Liu, G. Chen, G. Liu, B. Ren and Z. Tian, *J. Phys. Chem. Lett.*, 2020, **11**, 1022–1029.
- 24 L. A. Wijanayaka, M. R. Ivanov, C. M. Cheatum and A. J. Haes, *J. Phys. Chem. C*, 2015, **119**, 10064–10075.
- 25 S. L. Kleinman, R. R. Frontiera, A. I. Henry, J. A. Dieringer and R. P. Van Duyne, *Phys. Chem. Chem. Phys.*, 2013, **15**, 21–36.
- 26 Z. Yang, Q. H. Li, F. X. Ruan, Z. P. Li, B. Ren, H. X. Xu and Z. Q. Tian, *Chin. Sci. Bull.*, 2010, **55**, 2635–2642.
- 27 D. M. Solis, J. M. Taboada, F. Obelleiro, L. M. Liz-Marzán and F. J. G. Abajo, *ACS Photonics*, 2017, **4**, 329–337.
- 28 H. H. Liu, S. Surawanvijit, R. Rallo, G. Orkoulas and Y. Cohen, *Environ. Sci. Technol.*, 2011, **45**, 9284–9292.
- 29 R. Chen, L. Zhang, X. Li, L. Ong, Y. G. Soe, N. Sinsua, S. L. Gras, R. F. Tabor, X. Wang and W. Shen, *ACS Sens.*, 2017, **2**, 1060–1067.
- 30 T. Andryszewski, M. Iwan, M. Holdyński and M. Fiałkowski, *Chem. Mater.*, 2016, **28**, 5304–5313.
- 31 M. D. Hernando, M. Mezcuca, A. R. Fernandez-Alba and D. Barcelo, *Talanta*, 2006, **69**, 334–342.
- 32 X. Ye and J. Liu, *Environ. Pollut.*, 2019, **245**, 590–599.
- 33 X. Chen, M. Lin, L. Sun, T. Xu, K. Lai, M. Huang and H. Lin, *Food Chem.*, 2019, **293**, 271–277.
- 34 P. Ma, L. Wang, L. Xu, J. Li, X. Zhang and H. Chen, *Eur. Food Res. Technol.*, 2020, **246**, 239–251.
- 35 L. Ouyang, P. Dai, L. Yao, Q. Zhou, H. Tang and L. Zhu, *Analyst*, 2019, **144**, 5528–5537.
- 36 H. Dies, A. Bottomley, D. L. Nicholls, K. Stamplecoskie, C. Escobedo and A. Docoslis, *Nanomaterials*, 2020, **10**, 661.
- 37 Q. Ding, J. Wang, X. Chen, H. Liu, Q. Li, Y. Wang and S. Yang, *Nano Lett.*, 2020, 0c02683.
- 38 P. Zhao, H. Liu, L. Zhang, P. Zhu, S. Ge and J. Yu, *ACS Appl. Mater. Interfaces*, 2020, **12**, 8845–8854.
- 39 M. Pastorello, F. A. Sigoli, D. P. dos Santos and I. O. Mazali, *Spectrochim. Acta, Part A*, 2020, **231**, 118113.
- 40 H. Sun, H. Liu and Y. Wu, *Appl. Surf. Sci.*, 2017, **416**, 704–709.
- 41 S. Pang, T. P. Labuzab and L. He, *Analyst*, 2014, **139**, 1895.
- 42 M. V. Gorbachevskii, D. S. Kopitsyn, M. S. Kotelev, E. V. Ivanov, V. A. Vinokurov and A. A. Novikov, *RSC Adv.*, 2018, **8**, 19051.